Chinese Chemical Letters 34 (2023) 108527

Contents lists available at ScienceDirect

Chinese Chemical Letters

journal homepage: www.elsevier.com/locate/cclet

Low temperature, non-halogen solvent processed single-component organic solar cells with 10% efficiency

Zhou Zhang[a,1], Jing Wang[b,1], Zhijie Hu[a], Chengyi Xiao[a], Qiaomei Chen[a,*], Zheng Tang[b,*], Weiwei Li[a,*]

[a] Beijing Advanced Innovation Center for Soft Matter Science and Engineering & State Key Laboratory of Organic-Inorganic Composites, Beijing University of Chemical Technology, Beijing 100029, China
[b] Center for Advanced Low-dimension Materials, College of Materials Science and Engineering, Donghua University, Shanghai 201620, China

ARTICLE INFO

Article history:
Received 17 March 2023
Revised 26 April 2023
Accepted 27 April 2023
Available online 30 April 2023

Keywords:
Organic solar cells
Non-halogenated solvents
Double-cable conjugated polymers
Long-branched alkyl chains
Solubility

ABSTRACT

A double-cable conjugated polymer DCPIC-BO is designed *via* introducing a long-branched alkyl chains 2-buthyloctyl into the acceptor side unit. Compared with the double-cable polymer (DCPIC-EH) with the 2-ethylhexyl alkyl chains, the solubility of the DCPIC-BO in non-halogen solvents is substantially improved. Therefore, a power conversion efficiency (PCE) of 9.77% can be obtained by the devices processed from *o*-xylene at 40 °C, while the DCPIC-EH cannot be processed due to its poor solubility under this condition. Moreover, PCEs of 10.10% for small-area (0.04 cm^2) devices and nearly 9% for devices with an area of 1 cm^2 are achieved using a non-halogenated solid additive in *o*-xylene, realizing the "absolutely halogen-free" OSC fabrication.

© 2023 Published by Elsevier B.V. on behalf of Chinese Chemical Society and Institute of Materia Medica, Chinese Academy of Medical Sciences.

Organic solar cells (OSCs) are a type of photovoltaic cells that use the organic conjugated materials as the photoactive materials. They show huge potential for commercial applications owing to the advantages of abundant raw materials, high flexibility, semi-transparency, compatibility with low-cost large-area printing [1–11]. Thanks to the development of the photoactive materials (especially the Y-series acceptors), morphological control strategies, interlayer and device engineering, the power conversation efficiencies (PCEs) of OSCs have surpassed 19% [12–15]. However, the toxic halogenated solvents such as chloroform (CF), chlorobenzene (CB), and 1,2-dichlorobenzene (*o*-DCB) are always the best candidates for photoactive layer processing during the laboratory production of state-of-the-art OSCs devices. These toxic solvents pose serious threats to human health and the environment, constituting one of the major challenges in scaling up production of OSCs for industrial applications [16,17].

The use of non-halogenated solvents eliminates potential health and safety concerns associated with the use of halogenated solvents, making the fabrication process safer for workers and the environment [18–20]. Nevertheless, the poor solubility of present photoactive materials in non-halogenated solvents leads to suboptimal morphologies, thereby significantly impacting their performance [21,22]. To address this issue, numerous molecular design strategies and processing techniques have been proposed by researchers to enhance the compatibility between photoactive materials and non-halogenated solvents. For example, Dong *et al.* synthesized an efficient acceptor, known as DTY6, with longer alkyl chains (2-decyltetradecyl) compared to Y6 [23]. The PM6:DTY6 devices showed an obvious improvement of PCE (16.1%) compared to the PM6:Y6 counterparts (10.8%) when processing in *o*-xylene (*o*-XY), owing to the restricted aggregation and reasonable domain size of DTY6 in the blends [23]. In addition, Song *et al.* used a mixed halogen-free solvent of carbon disulfide (CS_2) and *o*-XY with the volume ratio of 7:3 to fabricated PM6:Y6-based OSC devices [24]. This approach yielded a high PCE of 16.5%, surpassing its counterparts processed with neat *o*-XY (13.3%). This is due to the mixed solvent that effectively increases the solubility and miscibility of PM6 and Y6, resulting in the optimal phase separation and proper aggregation domains within the active layer. Furthermore, a recent study by Daniel *et al.* developed a set of terpene-based binary solvent systems according to the Hansen solubility parameters (HSP), which were found to be both effective and environmentally friendly for a range of organic electronics devices [25]. Despite of the success achieved, the processing of bulk-heterojunction OSCs using non-halogen solvents remains a complicated and demanding task. Since the material nature of the polymer donors and the small molecule acceptors are distinct [26,27], the selection of

* Corresponding authors.
E-mail addresses: chenqm@mail.buct.edu.cn (Q. Chen), ztang@dhu.edu.cn (Z. Tang), liweiwei@iccas.ac.cn (W. Li).
[1] These authors contributed equally to this work.

https://doi.org/10.1016/j.cclet.2023.108527
1001-8417/© 2023 Published by Elsevier B.V. on behalf of Chinese Chemical Society and Institute of Materia Medica, Chinese Academy of Medical Sciences.

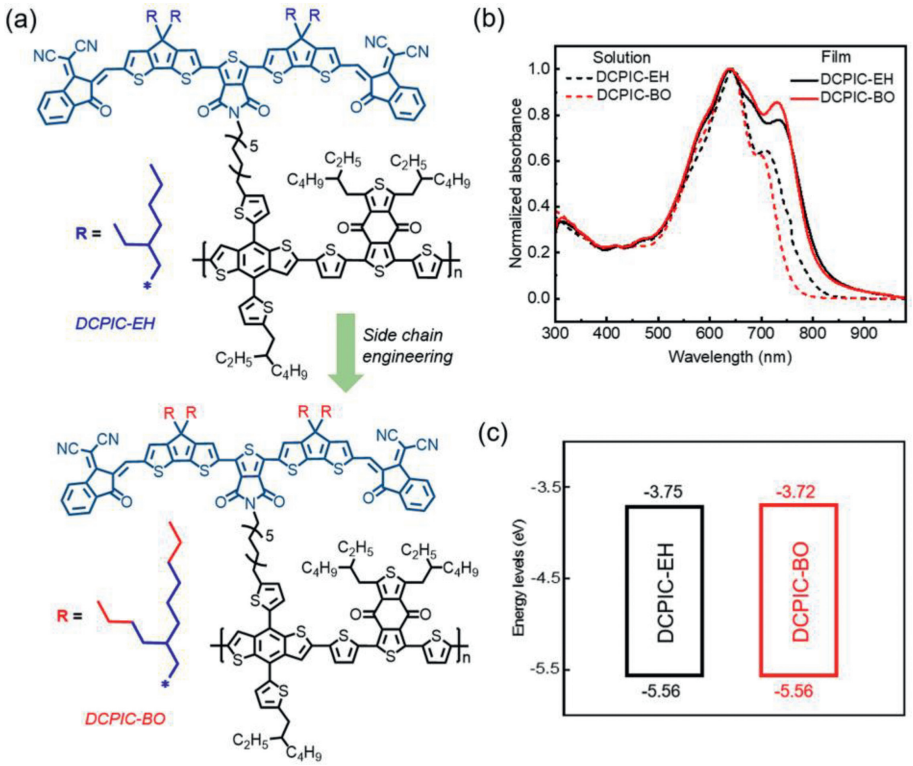

Fig. 1. Chemical structures, absorption spectra and energy level diagram of DCPIC-EH and DCPIC-BO. (a) Schematic diagram showing the designed double-cable conjugated polymer DCPCI-BO from DCPIC-EH *via* side chain engineering. (b) Optical absorption spectra in *o*-XY solution and corresponding thin films. (c) Energy level diagram.

non-halogenated solvents for processing should take a comprehensive consideration of the effects of material solubility and solvent volatility on the aggregation state and phase separation [23,24,28].

Double-cable conjugated polymers [29–35] are a type of polymers where the acceptor units are covalently bonded to the donor main chain, commonly utilized in the fabrication of single-component organic solar cells (SCOSCs), leading to a simpler and more cost-effective manufacturing process. Recently, our group took the lead in synthesizing double-cable conjugated polymers with non-fused near-infrared (NIR) acceptors for use in SCOSCs, which delivered a high PCE of 10.09% [36]. Nevertheless, the new double-cable polymers named as DCPIC-EH can only dissolved in hot *o*-dichlorobenzene (*o*-DCB) solvent to prepare high-performance SCOSC devices. In this work, we designed a new double-cable polymer (DCPIC-BO) with long-branched alkyl chains (2-buthyloctyl, BO) on the TPDIC (1,3-bis(4,4-bis(2-buthyloctyl)-4*H*-cyclopenta[1,2-*b*:5,4-*b*']dithiophen-2-yl)-5-(2-octyl)-4*H*-thieno[3,4-*c*]pyrrole-4,6(5*H*)–dione) acceptor side units (Fig. 1a). The solubility of DCPIC-BO was substantially improved in both the halogen and non-halogen solvents, compared with DCPIC-EH. As a result, the DCPIC-BO-based devices processed using either halogen or non-halogen solvents (CB, *o*-XY, and THF) at a mild temperature of 40 °C demonstrate similar PCEs of ~9.7%. In stark contrast, DCPIC-EH exhibits poor solubility in *o*-XY and THF at low temperature, impeding its processing with non-halogen solvents. In addition, we found that 2-methylanisole (2-MA) and a mixed solvent of eucalyptol (Eu) and tetralin (Tet) also can be utilized as alternative non-halogen processing solvents for DCPIC-BO to fabricate highly efficient SCOSCs devices. Furthermore, we employed a solid additive (SAD) to prepare "absolutely halogen-free" SCOSCs devices. This approach enabled high PCEs exceeding 10% for small-area (0.04 cm^2) devices and nearly 9% for devices with an area of 1 cm^2.

As shown in Fig. 1a, the new double-cable polymer DCPIC-BO was synthesized by extending the alkyl chain on TPDIC acceptor side unit of DCPIC-EH that was previously reported [36] from 2-ethylhexyl (EH) to 2-butyloctyl (BO) (The detailed synthesis and characterizations can be found in Supporting information). The gel permeation chromatography measurement shows that the number-average molecular weight (M_n) of DCPIC-BO is 34.8 kDa (Fig. S1 in Supporting information), which is lower than that of DCPIC-EH (93.1 kDa) [36]. Despite our attempts to synthesize several batches of DCPIC-BO, we were unable to achieve a high M_n comparable to that of DCPIC-EH. This has puzzled us for a considerable period, and we intend to investigate the underlying reasons in more detail.

The ultraviolet-visible (UV–vis) absorption spectra of the DCPIC-EH and DCPIC-BO in dilute *o*-XY (a widely used non-halogen solvent with moderate boiling point and excellent dissolving ability) solutions and thin films are shown in Fig. 1b. The absorption spectrum of DCPIC-BO in solution shows obvious blue shift (~37 nm) compared with that of DCPIC-EH, revealing the decrease in aggregation of DCPIC-BO in *o*-XY. The absorption spectra of DCPIC-BO in CB and THF are also presented in Fig. S2a (Supporting information), which further verify the enhanced solubility of DCPIC-BO in non-halogen solvents. When converted from the solution state to the thin films, the absorption profiles of the two polymers exhibit similar trends within the 400–900 nm range with the absorbance edge of DCPIC-BO slightly blue-shifted by ~9 nm relative to that of DCPIC-EH, which can be attributed to the steric hindrance effect of a long-branched alkyl chain in DCPIC-BO that results in the increase of laminar spacing. Despite of the slight blue shift, the DCPIC-BO film shows a superior aggregation, which is indicated by an increased ratio between the 0–0/0–1 peaks and due to the superior solubility of DCPIC-BO in *o*-XY that contributes to a favorable morphology. Further, the effect of alkyl chain on the fron-

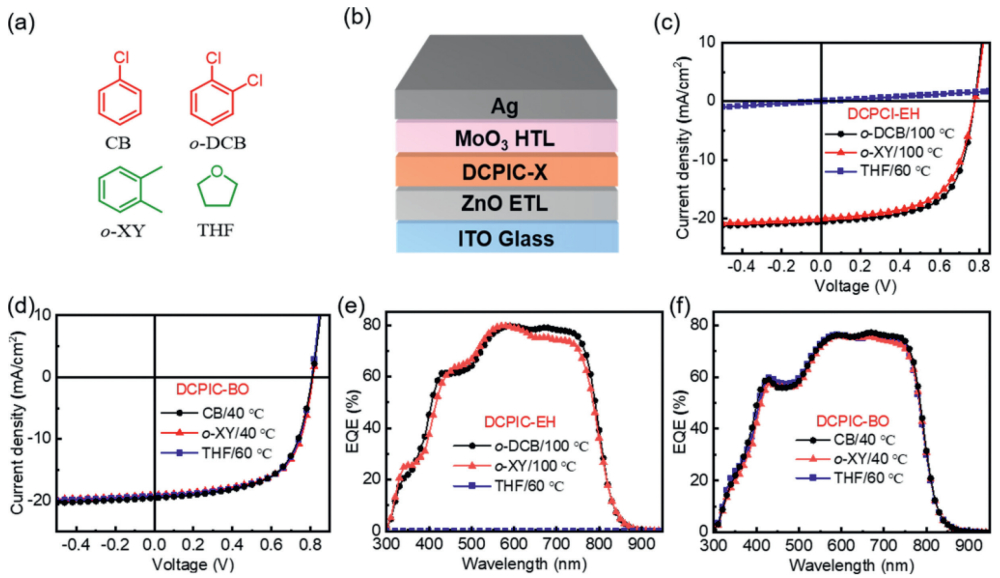

Fig. 2. (a) Molecule structures of CB, *o*-DCB and *o*-XY, THF solvents. (b) Scheme of devices configuration. *J-V* curves of (c) DCPIC-EH and (d) DCPIC-BO-based devices processed with various solvents. (e, f) The corresponding EQE plots.

tier energy levels of the two polymers were determined by cyclic voltammogram (CV) measurements, as shown in Fig. S3 (Supporting information) and Fig. 1c. Specifically, DCPIC-BO and DCPIC-EH display identical highest occupied molecular orbital (HOMO) energy levels of −5.56 eV, while the lowest unoccupied molecular orbital (LUMO) energy level of DCPIC-BO (−3.72 eV) is slightly upshifted from that of DCPIC-EH (−3.75 eV), which is considered to help in achieving a higher open-circuit voltage (V_{oc}) when manufacturing SCOSC devices.

Then, the solubility of DCPCI-EH and DCPIC-BO in various commonly used solvents for processing organic solar cells was investigated, including halogenated and non-halogenated solvents, such as *o*-DCB, CB, *o*-XY and THF. The chemical structures of these solvents are illustrated in Fig. 2a. Fig. S4 shows pictures of the two polymers dissolved in different solvents (10 mg/mL, the lowest concentration for proper photoactive layer thickness) and the corresponding thin films. It can be found that DCPIC-EH exhibits exiguous solubility (<1 mg/mL) in *o*-XY and THF at moderate temperatures (40 °C), resulting in severe aggregation and poor film quality. Following continuous heating of the solution on a hot stage, the solubility of DCPIC-EH in *o*-DCB and *o*-XY was enhanced, while remaining slightly soluble in THF. As anticipated, the long alkyl side chains in DCPIC-BO contribute to its excellent solubility in CB, *o*-XY, and THF, at both moderate and high temperatures, thereby enabling its solution processing into uniform and flat films.

To check the photovoltaic performance of the DCPIC-EH and DCPIC-BO processed from the above solutions, the SCOSCs devices with an inverted configuration of glass/ITO/ZnO/active layer/MoO_3/Ag were fabricated, as depicted in Fig. 2b. 1,8-Diiodooctane (DIO) was used to optimize the morphology of polymer films. Firstly, the optimal temperature to prepare the polymer solutions with different solvents were investigated. As shown in Figs. S5a and b and Table S1 (Supporting information), for DCPIC-EH-based devices, the optimal performance was obtained by the *o*-DCB solution with a temperature of 100 °C, showing an impressive PCE of 10.03%, a V_{oc} of 0.775 V, a short-circuit current density (J_{sc}) of 20.55 mA/cm^2 and a fill factor (FF) of 63.04%, while devices processed from *o*-XY solution under 100 °C yielded a decreased PCE of 9.36%. Notably, it was observed that when the temperature of the polymer solutions of *o*-DCB and *o*-XY is at 70 °C, the PCEs are significantly reduced to 8.84% and 2.30%, respectively. Furthermore, the low solubility of DCPIC-EH in *o*-XY (40 °C) and in THF at either 40 °C or 60 °C makes it difficult to obtain working devices. However, when replacing DCPIC-EH by DCPIC-BO, the solvent and temperature dependence is significantly reduced. As shown in Figs. S5c and e and Table S2 (Supporting information), regardless of whether the processing solvent is CB or *o*-XY and whether the solution temperature is 40 °C or 100 °C, the resulting devices exhibit closed PCE values around 9.7%. Even processed from THF, a PCE of 9.76% can be achieved at solution temperature of 60 °C and only slightly decreases to 8.32% at 40 °C. The current density-voltage (*J-V*) curves and external quantum efficiency (EQE) spectra for the best devices processed from different solvents are shown in Figs. 2c-f and the corresponding photovoltaic parameters are summarized in Table 1. The higher V_{oc}s exhibited by the DCPIC-BO-based devices compared with those based on DCPIC-EH can be attributed to the reduction in non-radiative charge carrier decay resulting from the increased donor-acceptor spacing facilitated by the long-branched alkyl chain in DCPIC-BO [37]. All the above results indicate that the long-branched alkyl chain enhance the solubility of DCPIC-BO in different solvents, either halogenated or non-halogenated solvents, enabling the solution processing at both moderate and high temperatures to achieve high photovoltaic performance.

Further, atomic force microscopy (AFM) was carried out to detect the surface morphologies and phase separation of DCPCI-BO films processed from CB, *o*-XY and THF. As shown in Fig. S6 (Supporting information), the surface roughness (RMS) of *o*-XY and THF processed DCPIC-BO films were 0.63 nm and 0.56 nm, respectively, which were comparable to that processed from CB solution. Moreover, the DCPIC-BO films processed from CB, *o*-XY and THF all exhibit delicate phase separation, which is consistent with the results of *o*-DCB processed DCPIC-EH in our previous reports [36]. Also, grazing incidence wide-angle X-ray scattering (GIWAXS) was applied to study the molecular packing and crystalline behaviors of the DCPIC-BO films. The 2D GIWAXS images of CB, *o*-XY and THF processed DCPIC-BO films and the corresponding 1D in-plane (IP) and out-of-plane (OOP) plots are shown in Fig. 3 and the crystalline parameters are summarized in Table S4 (Supporting information). It reveals that, compared with the film processed from CB, similar face-on orientation and crystallinity can be obtained by both *o*-XY and THF processed films, which was further verified

Table 1
Photovoltaic parameters of the devices processed from different solvents.

Active layer	Solvent / Temperature [a]	V_{oc} (V)	J_{sc} [b] (mA/cm^2)	J_{cal} [c] (mA/cm^2)	FF (%)	PCE [d] (%)
DCPIC-EH	*o*-DCB / 100 °C	0.775 (0.770 ± 0.003)	20.55 (20.30 ± 0.21)	19.60	63.04 (62.67 ± 0.81)	10.03 (9.86 ± 0.21)
	o-XY / 100 °C	0.775 (0.771 ± 0.002)	20.04 (19.77 ± 0.31)	19.13	60.21 (59.24 ± 0.92)	9.36 (9.03 ± 0.24)
	THF / 60 °C	–	–	–	–	–
DCPIC-BO	CB / 40 °C	0.810 (0.810 ± 0.001)	19.55 (19.29 ± 0.17)	18.57	61.22 (60.92 ± 0.42)	9.70 (9.52 ± 0.15)
	o-XY / 40 °C	0.812 (0.809 ± 0.002)	19.08 (19.15 ± 0.10)	18.15	62.97 (61.96 ± 0.72)	9.77 (9.60 ± 0.11)
	THF / 60 °C	0.808 (0.809 ± 0.001)	19.30 (19.22 ± 0.09)	18.40	62.56 (60.71 ± 0.68)	9.76 (9.44 ± 0.21)

[a] The temperature of heating stage is regarded as the solution temperature.
[b] The device area is 4.00 mm^2.
[c] Calculated integral current density from EQE spectra and match well with J_{sc} within 5% error.
[d] Average values from 8 independent cells in parentheses.

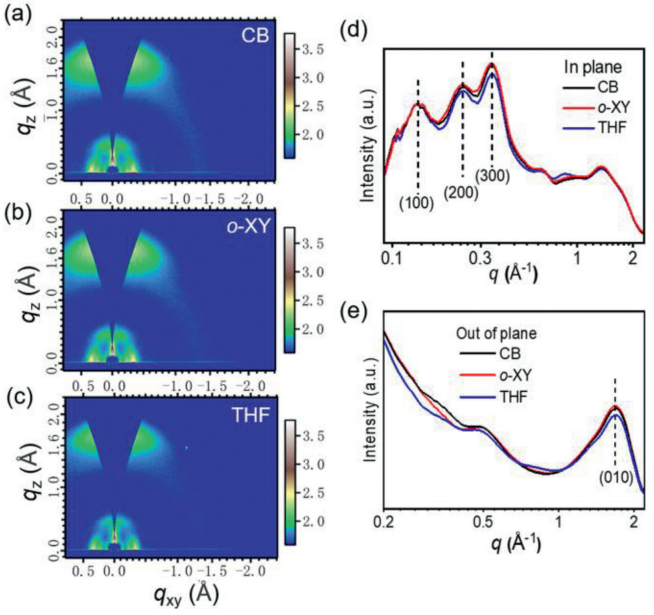

Fig. 3. 2D GIWAXS images of (a) CB, (b) *o*-XY and (c) THF-processed DCPIC-BO films. (d) In-plane and (e) out of plane 1D plots of the corresponding GIWAXS images.

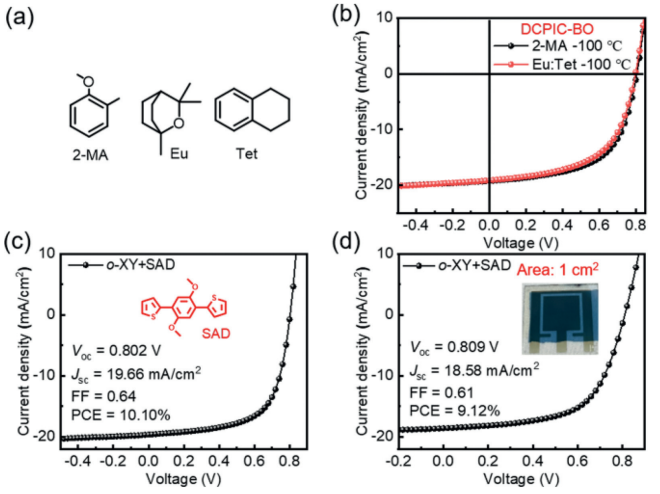

Fig. 4. (a) The molecular structure of 2-MA, Eu and Tet. (b) *J-V* curves of DCPIC-BO processed from 2-MA, Eu and Tet. (c) *J-V* curves of DCPIC-BO-based small-area (0.04 cm^2) devices processed from o-XY with SAD solid additive. (d) *J-V* curves of DCPIC-BO-based devices with 1 cm^2 area.

by the pretty similar optical absorption spectra of films processed from CB, *o*-XY and THF solutions (Fig. S2b in Supporting information).

Moreover, we investigated whether DCPIC-BO can be processed by other non-halogenated solvents. Surprisingly, solvents including 2-MA, Eu and Tet (Fig. 4a) also shows capability of solution processing of DCPIC-BO. Specifically, 2-MA-based devices exhibit an optimal PCE of 9.11% with a V_{oc} of 0.805 V, a J_{sc} of 19.23 mA/cm^2 and an FF of 58.80%, as well as obtaining an efficiency of 8.60% by using a mixed solvent recipe of Eu and Tet as reported in the literature (Table S3 in Supporting information, Fig. 4b) [25].

Furthermore, to address the non-environmental friendliness of DIO, we substituted DIO with a non-halogen solid additive (SAD, inset of Fig. 4c) in *o*-XY to produce completely halogen-free DCPCI-BO-based devices [38]. The SAD-based small-area (0.04 cm^2) devices exhibited a remarkable efficiency of 10.10% (Fig. 4c), and devices with an area of 1 cm^2 achieved an efficiency of 9.12% (Fig. 4d). These results confirm that the double-cable conjugated polymer DCPIC-BO is an efficient organic photovoltaic material that can be processed using non-halogen solvents.

In this work, we synthesized a double-cable conjugated polymer (DCPIC-BO) by extending the alkyl side chains of the acceptor side units in DCPIC-EH and utilized as the light-absorbing material in solution-processed SCOSCs. The results demonstrate that DCPIC-BO-based devices processed from either halogen or non-halogen solvents (CB, *o*-XY, and THF) at a mild temperature of 40 °C exhibit comparable PCEs of ~9.7%. In contrast, DCPIC-EH cannot be solution-processed in *o*-XY and THF at low temperatures. DCPI-EH is soluble in *o*-XY at 100 °C, yet the efficiency of *o*-XY-processed devices (9.36%) is still lower than that of *o*-DCB (10.03%). AFM and GIWAXS analyses suggest that the DCPIC-BO treated with non-halogen solvents results in an ideal film morphology, similar to that obtained with halogen solvents. Moreover, DCPIC-BO can be treated with other non-halogen solvents, such as 2-MA, Eu, and Tet. Of particular significance is that *o*-XY-processed DCPIC-BO devices fabricated with a non-halogen solid additive (SAD) achieve a high PCE of 10.1%. This work not only presents a double-cable conjugated polymer with the advantages of non-halogen solvent processing, but also provides a straightforward approach to modify conjugated polymers for achieving environmentally friendly manufacturing.

Declaration of competing interest

The authors declare that they have no known competing financial interests or personal relationships that could have appeared to influence the work reported in this paper.

Acknowledgments

This study is jointly supported by Beijing Natural Science Foundation (Nos. JQ21006 and 2212045) and National Natural Science Foundation of China (NSFC, Nos. 52073016 and 92163128). This work was further supported by the Fundamental Research Funds

for the Central Universities (Nos. buctrc202111, buctrc201828 and XK1802-2), and the Opening Foundation of State Key Laboratory of Organic-Inorganic Composites of Beijing University of Chemical Technology (No. oic-202201006).

Supplementary materials

Supplementary material associated with this article can be found, in the online version, at doi:10.1016/j.cclet.2023.108527.

References

[1] L.Y. Lu, T.Y. Zheng, Q.H. Wu, et al., Chem. Rev. 115 (2015) 12666–12731.
[2] X.Y. Dong, Y.Y. Jiang, L.L. Sun, et al., Adv. Funct. Mater. 32 (2022) 2110209.
[3] F. Qin, L.L. Sun, H.T. Chen, et al., Adv. Mater. 33 (2021) 2103017.
[4] Y.P. Wang, Q.M. Chen, G.C. Zhang, et al., Chem. Eng. J. 451 (2023) 138612.
[5] K. Fukuda, K. Yu, T. Someya, Adv. Energy Mater. 10 (2020) 2000765.
[6] G. Zeng, W.J. Chen, X.B. Chen, et al., J. Am. Chem. Soc. 144 (2022) 8658–8668.
[7] C.C. Xie, C.Y. Xiao, J. Fang, et al., Nano Energy 107 (2023) 108153.
[8] G.C. Zhang, Q.M. Chen, C.C. Xie, et al., npj Flex. Electron. 6 (2022) 37.
[9] B.Q. Liu, Y.H. Xu, D.D. Xia, et al., Acta Phys. Chim. Sin. 37 (2021) 2009056.
[10] X.Y. Xu, H.B. Wu, S.J. Liang, et al., Acta Phys. Chim. Sin. 38 (2022) 2201039.
[11] Y.Y. Zhou, M. Li, Hao. Lu, et al., Adv. Funct. Mater. 31 (2021) 2101742.
[12] Y.N. Wei, Z.H. Chen, G.Y. Lu, et al., Adv. Mater. 34 (2022) 2204718.
[13] L. Zhu, M. Zhang, J.Q. Xu, et al., Nat. Mater. 21 (2022) 656–663.
[14] Y. Cui, Y. Xu, H.F. Yao, et al., Adv. Mater. 33 (2021) 2102420.
[15] C.L. He, Y.W. Pan, Y. Ouyang, et al., Energy Environ. Sci. 15 (2022) 2537–2544.
[16] C. Capello, U. Fischer, K. Hungerbühler, Green Chem. 9 (2007) 927–934.
[17] V. Hessel, N.N. Tran, M.R. Asrami, et al., Green Chem. 24 (2022) 410–437.
[18] X.F. Chen, X.F. Liu, M.A. Burgers, et al., Angew. Chem. Int. Ed. 53 (2014) 14378–14381.
[19] S.T. Pang, Z.L. Chen, J.Y. Li, et al., Mater. Horiz. 10 (2023) 473–482.
[20] J. Guo, Y. Wu, W. Wang, T. Wang, J. Min, Sol. RRL 6 (2022) 2101024.
[21] S.Q. Zhang, L. Ye, H. Zhang, et al., Mater. Today 19 (2016) 533–543.
[22] S. Lee, D. Jeong, C. Kim, et al., ACS Nano 14 (2020) 14493–14527.
[23] S. Dong, T. Jia, K. Zhang, et al., Joule 4 (2020) 2004–2016.
[24] X. Song, P. Sun, D.W. Sun, et al., Nano Energy 91 (2022) 106678.
[25] D. Corzo, D. Rosas-Villalva, C. Amruth, et al., Nat. Energy 8 (2023) 62–73.
[26] W. Liu, X. Xu, J. Yuan, et al., ACS Energy Lett. 6 (2021) 598–608.
[27] Z. Zheng, H.F. Yao, L. Ye, et al., Mater. Today 35 (2020) 115–130.
[28] B. Liu, H.L. Sun, J.W. Lee, et al., Energy Environ. Sci. 14 (2021) 4499–4507.
[29] D. Wang, Z.F. Yang, F. Liu, et al., Chin. Chem. Lett. 33 (2022) 466–469.
[30] X.D. Jiang, J.J. Yang, S. Karuthedath, et al., Angew. Chem. Int. Ed. 59 (2020) 21683–21692.
[31] G.T. Feng, W.L. Tan, S. Karuthedath, et al., Angew. Chem. Int. Ed. 60 (2021) 25499–25507.
[32] G.T. Feng, J.Y. Li, Y.K. He, et al., Joule 3 (2019) 1765–1781.
[33] B.Q. Liu, Y.H. Xu, F. Liu, et al., Chin. J. Polym. Sci. 40 (2022) 898–904.
[34] S.J. Liang, C.Y. Xiao, C.C. Xie, et al., Adv. Mater. 35 (2023) 2300629.
[35] W.B. Lai, S. Karuthedath, C.Y. Xiao, et al., Chin. Chem. Lett. (2023), doi:10.1016/j.cclet.2023.108287.
[36] S.J. Liang, B.Q. Liu, S. Karuthedath, et al., Angew. Chem. Int. Ed. 61 (2022) 202209316.
[37] J. Wang, X.D. Jiang, H.B. Wu, et al., Nat. Commun. 12 (2021) 6679.
[38] C.Q. Li, X.B. Gu, Z.H. Chen, et al., J. Am. Chem. Soc. 144 (2022) 14731–14739.